Asian Journal of Current Research in Clinical Cancer
2022, Volume 2, Issue 1, Page No: 25-33

Available online at: www.galaxypub.co/page/journals

Galaxy Publication

Computational Evaluation of Dibenzo Compounds as Potential Dual Inhibitors of Androgen Receptor and 5α-Reductase

Lauro FigueroaValverde[1], Marcela Rosas-Nexticapa[2], Magdalena AlvarezRamirez[2], Maria Lopez-Ramos[1], Virginia MateuArmand[2]*

[1]Pharmacochemistry Research Laboratory, Faculty of BiologicalChemical Sciences, University Autonomous of Campeche; Humberto Lanz Cárdenas s/n, Ex Hacienda Kalá, C.P. 24085, Campeche, Mexico.
[2]Nutrition Laboratory, Faculty of Nutrition, University of Veracruz, Medicos y s/n Odontologos 910210, Unidad del Bosque, Xalapa, Mexico.

***E-mail** ✉ lfiguero@uacam.mx

Received: 04 March 2022; **Revised:** 23 May 2022; **Accepted:** 25 May 2022

ABSTRACT

While various drugs are available for the treatment of cancer, many of them are associated with side effects such as high blood pressure, liver damage, and erectile dysfunction. In the search for safer treatment options, some dibenzo derivatives have shown potential against cancer. However, conflicting reports indicate that certain dibenzo compounds might worsen the disease. This inconsistency could be due to structural differences among the dibenzo derivatives. To clarify this, the present study investigated the potential interactions of 15 dibenzo derivatives (compounds 1–15) with biomolecular targets linked to prostate cancer—specifically, the androgen receptor and the 5α-reductase enzyme. Molecular docking analysis was performed using known reference drugs, including flutamide, dutasteride, and finasteride. The findings showed that compounds 9, 11, and 15 may bind to the androgen receptor, while compounds 2, 5, and 13 showed potential interactions with the 5α-reductase enzyme. These results suggest that certain dibenzo derivatives could serve as promising candidates for the development of novel prostate cancer therapies.

Keywords: Dibenzo, Cancer, Androgen, 5α-reductase

How to Cite This Article: FigueroaValverde L, Rosas-Nexticapa M, AlvarezRamirez M, Lopez-Ramos M, MateuArmand V. Computational Evaluation of Dibenzo Compounds as Potential Dual Inhibitors of Androgen Receptor and 5α-Reductase. Asian J Curr Res Clin Cancer. 2022;2(1):25-33.

Introduction

Prostate cancer remains one of the leading causes of death among men globally. Its incidence has been rising in recent years, closely linked to the aging male population [1]. Current treatment strategies include drugs targeting the androgen receptor—such as flutamide [2], nilutamide [3], bicalutamide [4], enzalutamide [5], and apalutamide [6]—as well as 5α-reductase inhibitors like finasteride [7] and dutasteride [8]. However, many of these drugs are associated with adverse side effects, including hot flashes [9], hypertension [10], liver damage [11], and erectile dysfunction [12].

In the ongoing search for safer and more effective alternatives, several novel compounds have been developed. For example, ERGi-USU-6, derived from ERGi-USU, has been proposed as an ERG protein inhibitor for prostate cancer therapy [13]. Other promising candidates include Y08060, a BRD4 inhibitor [14], and a range of 1,4-substituted triazoles with antiandrogenic activity [15]. Additional research has explored quercetin-based phosphatidylinositol-3-kinase inhibitors like LY294002, as well as the Mu-LEHSSKLQL peptide, both of which induce apoptosis in C4-2 prostate cancer cells [16]. Trioxane dimers have also shown potential, causing G0/G1 phase cell cycle arrest in LNCaP prostate cancer cells [17]. More recently, AKR1C3 inhibitors such as carboxamide derivatives [18] and proteasome inhibitors like FPA-137, a quinolone thiosemicarbazone [19], have demonstrated activity against prostate cancer.

Several studies have highlighted the role of androgen receptor inhibition in reducing prostate cancer cell growth. For instance, lupeol has been identified as a natural androgen receptor antagonist [20], and certain curcumin analogs have shown similar antiandrogenic effects [21]. Moreover, JNJ-63576253 has been developed as a promising drug for treating castration-resistant prostate cancer through androgen receptor inhibition [22]. Hydroxylated dibenzo[b;d]pyran-6-one derivatives, known as urolithins, have also demonstrated antiproliferative activity against LNCaP cells, comparable to standard antiandrogen drugs [23].

These diverse findings suggest that multiple compounds can influence prostate cancer progression via distinct mechanisms, likely due to structural variations between molecules.

Therefore, the objective of this study was to evaluate the potential interaction of various dibenzo derivatives with key molecular targets involved in prostate cancer—the androgen receptor and the 5α-reductase enzyme—through molecular docking simulations using flutamide, dutasteride, and finasteride as reference drugs.

Materials and Methods

A total of fifteen dibenzo derivatives **(Figure 1)** were selected for this study to evaluate their potential interactions with two key biomolecular targets involved in prostate cancer: the androgen receptor and the 5α-reductase enzyme. The assessment was carried out using the following computational approach:

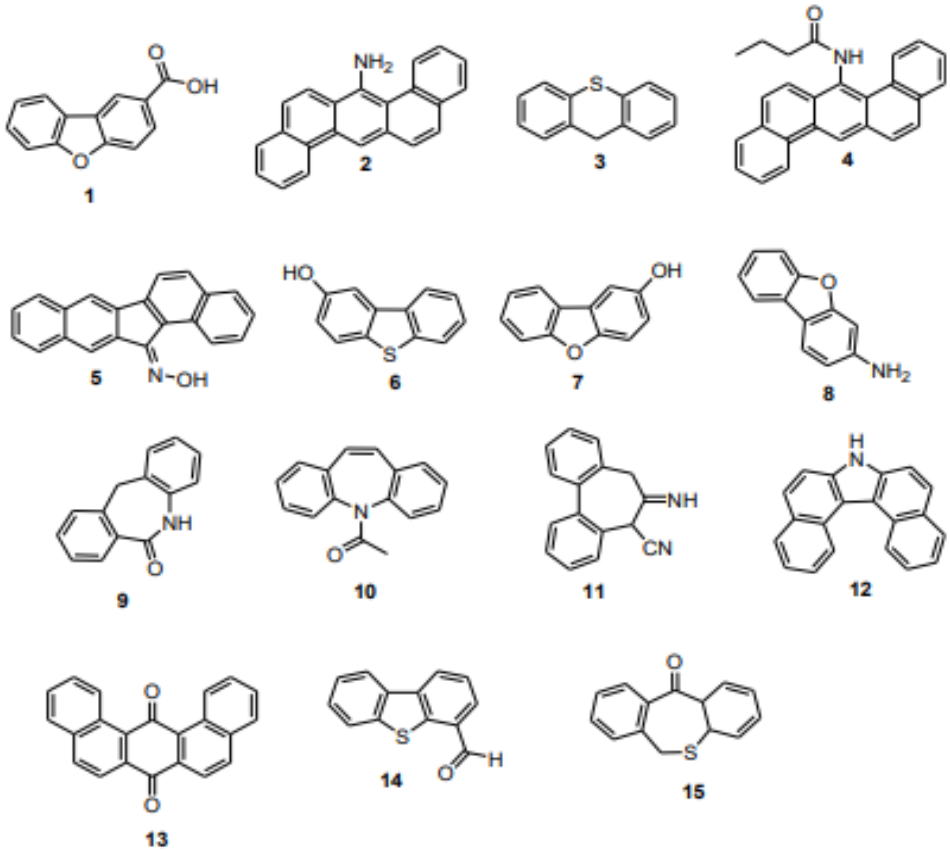

Figure 1. The chemical structures of dibenzo derivatives: 1) Dibenzo[b,d]furan-2-carboxylic acid [24], 2) 10H-Dibenzo[a,h]anthracen-7-ylamine [25], 3) 10H-Dibenzo[b,e]Thiopyran [26], 4) 1n-Dibenzo[a,h]anthracen-7-yl-Butamide [27], 5) 1n-Dibenzo[a,h]fluoren-13-one oxime [28], 6) 1n-Dibenzo[b,d]Thiophen-2-ol [29], 7) 1n-Dibenzo[b,d]furan-2-ol [30], 8) 1n-Dibenzo[b,d]furan-3-amine [31], 9) 5,11-Dihydro-6H-dibenzo[b,e]azepin-6-one [32], 10) 5-acetyl-5H-dibenzo[b,f]azepine [33], 11) 6-imino-6,7-dihydo-5H-dibenzo[a,c]cycloheptene-5-carbonitrile [34], 12) 7H-Dibenzo[c,g]carbazole [35], 13) Dibenzo[a,j]Anthracene-7,14-dione [36], 14) Dibenzo[b,d]thiophene-4-carbaldehyde [37], and 15) Dibenzo[b,e]thiepin-11(6H)-one [38].

Figure 1 shows the chemical structures of 15 dibenzo derivatives.

ligand-protein interaction

The binding interactions between the dibenzo derivatives and the androgen receptor as well as the 5α-reductase enzyme were examined using 4fdh [39] and 7bw1 [40] proteins as models. To identify the types of binding energies involved, the DockingServer software was employed for simulation and analysis [41].

Pharmacokinetic parameters

The pharmacokinetic properties of the compounds were analyzed using the SwissADME platform [42].

Toxicity assessment

The potential toxicity of Dibenzo[b,e]thiophen-11(6H)-one was evaluated using the GUSAR toxicity prediction tool [43].

Results and Discussion

Many studies have highlighted the anti-cancer potential of Dibenzo derivatives [44]. However, other research suggests that some Dibenzo derivatives may exhibit mutagenic effects in certain biological models [45]. This contradiction might stem from several factors, including:

1. Variations in the chemical structures of the Dibenzo derivatives.
2. The differing sites where these compounds act.
3. Disparities in concentrations and methods of administration.

Considering both the conflicting results and additional evidence, this study focused on how certain dibenzo-p-dioxins might increase prostate cancer risk through androgen receptor interaction [20-22]. The interaction of the 15 dibenzo derivatives with the androgen receptor was assessed using the 4fdh protein [39] and flutamide (a known androgen receptor inhibitor) [2] in a docking simulation model [41].

Table 1. Aminoacid residues are involved in the coupling of dibenzo derivatives (compounds 1-5) with the 4fdh protein surface.

Flutamide	Leu$_{701}$; Leu$_{704}$; Asn$_{705}$; Gln$_{711;}$ Trp$_{741;}$ Met$_{745;}$ Val$_{746}$; Met$_{749}$; Phe$_{764}$;Met$_{780}$; Met$_{787}$; Leu$_{873}$; Phe$_{876}$; Thr$_{877}$; Met$_{895}$
1	Leu$_{704}$; Asn$_{705}$; Gln$_{711}$; Met$_{745}$; Met$_{749}$; Arg$_{752}$; Phe$_{764}$; Met$_{895}$
2	Leu$_{701}$; Leu$_{704}$; Asn$_{705}$; Leu $_{707}$; Gln$_{711}$; Met$_{742}$; Met$_{745}$; Val$_{746}$; Met$_{749}$; Arg$_{752}$; Phe$_{764}$; Met$_{780}$; Leu$_{873}$; Phe$_{876}$; Thr$_{877}$
3	Asn$_{705}$; Leu$_{707}$; Gln$_{711}$; Met$_{742}$; Met$_{745}$; Met$_{749}$; Arg$_{752}$: Phe$_{764}$; Met$_{895}$
4	Leu$_{701}$; Leu$_{704}$; Asn$_{705}$; Leu $_{707}$; Trp$_{741}$; Met$_{745}$; Val$_{746}$; Met$_{749}$; Phe$_{764}$; Met$_{780}$; Met$_{787;}$ Leu$_{873}$; Phe$_{876}$; Thr$_{877}$; Leu$_{880}$; Met$_{895}$
5	Leu$_{701}$; Leu$_{704}$; Asn$_{705}$; Leu $_{707}$; Gln$_{711}$; Met$_{742}$; Val$_{746}$; Met$_{749}$; Arg$_{752}$; Phe$_{764}$; Met$_{780}$; Leu$_{873}$; Phe$_{876}$; Thr$_{877}$; Leu$_{880}$
6	Asn$_{705}$; Met$_{745}$; Val$_{746}$; Met$_{749}$; Phe$_{764}$; Met$_{787}$; Met$_{895}$
7	Leu$_{701}$; Leu$_{704}$; Asn$_{705}$; Leu $_{707}$; Phe$_{764}$; Met$_{780}$; Leu$_{873}$; Phe$_{876}$; Thr$_{877}$
8	Leu$_{704}$; Leu $_{707;}$ Gln$_{711}$; Met$_{745}$; Val$_{746}$; Met$_{749}$; Arg$_{752}$; Phe$_{764}$; Leu$_{873}$
9	Leu$_{704}$; Asn$_{705}$; Leu$_{707}$; Gln$_{711}$; Trp$_{741}$; Met$_{742}$; Met$_{745}$; Val$_{746}$; Met$_{749}$; Phe$_{764}$; Thr$_{877}$; Met$_{895}$
10	Leu$_{704}$; Leu$_{707}$; Gln$_{711}$; Trp$_{741}$; Met$_{742}$; Met$_{745}$; Val$_{746}$; Met$_{749}$; Arg$_{752}$; Phe$_{764}$; Met$_{780}$; Met$_{787}$; Leu$_{873}$
11	Leu$_{704}$; Leu$_{707}$; Gln$_{711}$; Met$_{742}$; Met$_{745}$; Val$_{746}$; Met$_{749}$; Phe$_{764}$; Met$_{780}$; Met$_{787}$; Leu$_{873}$
12	Leu$_{704}$; Asn$_{705}$; Leu$_{707}$; Gln$_{711}$; Val$_{746}$; Met$_{749}$; Phe$_{764}$; Met$_{780}$; Met$_{787}$; Leu$_{873}$; Thr$_{877;}$ Met$_{895}$
13	Asn$_{705}$; Leu$_{707}$; Gln$_{711}$; Met$_{742}$; Met$_{749}$; Arg$_{752}$; Phe$_{764}$; Met$_{780}$; Leu$_{873}$; Phe$_{876}$; Thr$_{877}$; Met$_{895}$
14	Asn$_{705}$; Leu$_{707}$; Gln$_{711}$; Val$_{746}$; Met$_{749}$; Arg$_{752}$; Phe$_{764}$; Met$_{787}$; Met$_{895}$
15	Leu$_{704}$; Asn$_{705}$; Leu$_{707}$; Gln$_{711}$; Met$_{742}$; Met$_{745}$; Val$_{746}$; Met$_{749}$; Arg$_{752}$; Phe$_{764}$

The results **(Table 1; Figure 2)** indicate that flutamide interacts with various amino acid residues on the 4fdh protein surface, in contrast to the interaction observed with the dibenzo derivatives (1 to 15). This suggests that

the variation in interaction is likely due to the different functional groups present in the chemical structures of each dibenzo derivative **(Tables 1-3; Figure 2)**.

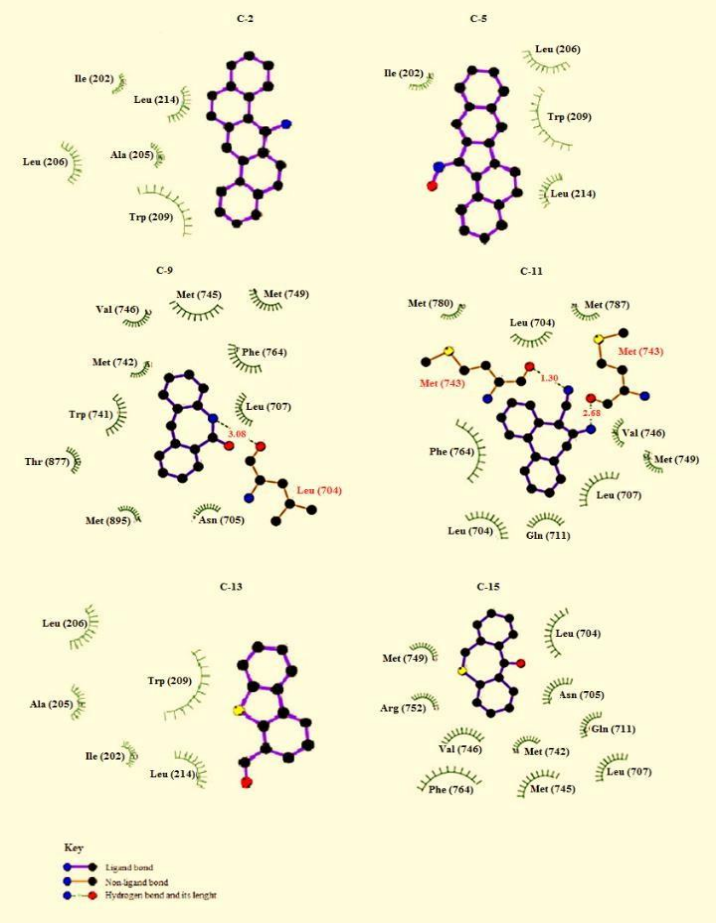

Figure 2. The diagram illustrates the binding sites of amino acid residues involved in the interaction of dibenzo derivatives (9, 11, and 15) with the 4fdh protein surface; additionally, compounds 11, 13, and 15 show potential interaction with the 7bw1 protein surface; visualization was done using GLmol viewer and DockingServer.

It is important to note that several studies highlight the significance of energy levels in protein-ligand interactions for determining the stability of the resulting protein-ligand complex. In this regard, several key factors should be taken into account: i) the free energy of binding, which quantifies the energy needed for a molecule to bind to a protein in an aqueous environment; ii) electrostatic energy, which is the result of the interaction between charges and electrostatic potential within the system; iii) the total intermolecular energy; and iv) van der Waals interactions, hydrogen bonds, and desolvation energy, which influence the behavior of water molecules within the protein-ligand system. In this study, we analyzed various thermodynamic parameters involved in the binding of Dibenzo derivatives to the 4fdh protein surface, using flutamide as a control androgen receptor inhibitor. The results **(Table 2)** revealed that compounds 9, 11, and 14 exhibited lower inhibition constants than flutamide and other derivatives (compounds 1-8, 10, and 12-14), suggesting they may interact more strongly with the 4fdh protein surface. This enhanced interaction could lead to modifications in androgen receptor activity, potentially reducing prostate cancer progression.

Table 2. Thermodynamic parameters involved in the interaction of dibenzo derivatives (1-15) and flutamide with the 4fdh-protein surface

Compound	A	B	C	D	E	F
Flutamide	-7.35	4.09	-8.51	-0.01	-8.51	443.01
1	-6.89	8.95	-6.87	-0.32	-7.19	410.76

2	-10.81	11.86	-11.09	-0.02	-11.11	530.21
3	-7.11	6.14	-7.11	+0.00	-7.11	400.69
4	-7.07	6.55	7.98	+0.01	-7.97	589.60
5	-9.77	68.60	-9.73	-0.34	-10.07	528.70
6	-6.55	15.79	-6.78	-0.07	-6.85	390.97
7	-5.83	53.23	-6.07	-0.06	-6.13	382.26
8	-6.83	9.77	-7.06	-0.07	-7.13	391.66
9	-7.65	2.47	-7.63	-0.02	-7.65	415.67
10	-8.27	859.79	-8.28	+0.01	-8.27	450.91
11	-8.03	1.29	-8.19	-0.14	-8.33	454.20
12	-10.10	39.73	-10.10	+0.00	-10.10	490.81
13	-8.48	612.25	-8.50	+0.02	-8.48	525.38
14	-7.14	5.89	-7.45	+0.01	-7.43	406.69
15	-8.03	1.31	-8.03	+0.00	-8.03	423.60

A = Est: free energy of binding (kcal/mol), B = Est. inhibition constant, Ki (mM), C = vdW + Hbond + desolv Energy (kcal/mol), D = electrostatic energy (kcal/mol), E = total Intermolec. energy (kcal/mol), and F = interact. surface

It is also crucial to highlight the involvement of other biomolecules, such as the 5α-reductase enzyme, in the development of prostate cancer. Research has suggested that certain dibenzo derivatives may affect the levels of the 5α-reductase enzyme in human prostate cancer cell lines. In this study, the potential effects of dibenzo derivatives were evaluated using the 7bw1 protein along with the drugs dutasteride and finasteride, which are known inhibitors of the 5α-reductase enzyme. The analysis, conducted with the DockingServer software, showed variations in the amino acid residues interacting with the dibenzo derivatives (compounds 1 to 15) in comparison to those involved in the interactions with dutasteride and finasteride **(Table 3; Figure 2)**.

Table 3. Aminoacid residues involved in the coupling of dibenzo derivatives (compounds 1-15) with 7bw1 protein surface.

Dutasteride	**Arg_{145}; Leu_{14}; Leu_{152}; Ile_{202}; Ala_{205}; Leu_{206}; Trp_{209}; Leu_{214}**
Finasteride	Tyr_{129}; Ile_{202}; Ala_{205}; Leu_{206}; Trp_{209}; Leu_{211}; Leu_{214}
1	Ala_{205}; Leu_{206}; Trp_{209}; Leu_{211}; Leu_{214}
2	Ile_{202}; Ala_{205}; Leu_{206}; Trp_{209}; Leu_{214}
3	Ala_{205}; Leu_{206}; Trp_{209}; Leu_{211}; Leu_{214}
4	Ile_{202}; Ala_{205}; Leu_{206}; Trp_{209}; Leu_{211}; Leu_{214}
5	Ile_{202}; Leu_{206}; Trp_{209}; Leu_{214}
6	Ala_{205}; Trp_{209}; Leu_{214}
7	Ala_{205}; Leu_{206}; Trp_{209}; Leu_{214}
8	Ile_{202}; Ala_{205}; Leu_{206}; Trp_{209}; Leu_{214}
9	Ile_{202}; Ala_{205}; Leu_{206}; Trp_{209}
10	Ala_{205}; Leu_{206}; Trp_{209}; Leu_{214}
11	Ile_{202}; Ala_{205}; Leu_{206}; Trp_{209}; Leu_{214}
12	Ala_{205}; Leu_{206}; Trp_{209}; Ser_{210}; Leu_{214}
13	Ala_{205}; Leu_{206}; Trp_{209}; Leu_{214}
14	Ile_{202}; Ala_{205}; Leu_{206}; Trp_{209}; Leu_{214}
15	Tyr_{129}; Ala_{134}; Tyr_{136}; Pro_{137}; Trp_{140}; Trp_{209}

In conclusion, the thermodynamic analysis of the dibenzo derivatives **(Table 4)** revealed that compound 13 exhibited a lower inhibition constant than finasteride. Additionally, compounds 2, 5, and 13 demonstrated distinct inhibition constant values when compared to dutasteride. These findings suggest that compounds 2, 5, and 13 may have a stronger affinity for the 7bw1 protein surface, potentially leading to enhanced inhibition of the 5α-reductase enzyme and, consequently, a reduction in prostate cancer progression.

Table 4. Thermodynamic parameters involved in the interaction of dibenzo derivatives (1-15), finasteride, and dutasteride with the 7bw1-protein surface.

Compound	A	B	C	D	E	F
Dutasteride	-9.81	64.59	-10.48	-0.03	-10.51	702.17
Finasteride	-7.48	3.30	-8.04	0.02	-8.02	639.91
1	-5.68	68.99	-5.95	-0.03	-5.98	450.84
2	-7.30	4.44	-7.60	-0.00	-7.60	533.59
3	-5.95	43.16	-5.97	0.01	-5.95	444.85
4	-6.92	8.40	-7.40	-0.00	-7.40	570.32
5	-7.39	3.84	-7.83	0.15	-7.69	539.21
6	-5.70	66.20	-6.00	0.01	-6.00	427.17
7	-4.99	218.52	-5.33	0.03	-5.29	424.95
8	-5.33	88.66	-5.83	0.01	-5.83	442.09
9	-5.98	41.23	-5.97	-0.01	-5.98	460.19
10	-6.11	33.33	-6.10	-0.00	-6.11	463.63
11	-5.05	200.14	-5.48	0.14	-5.35	463.14
12	-6.96	7.93	-6.94	-0.02	-6.96	470.67
13	-7.52	3.08	-7.52	0.01	-7.52	503.48
14	-5.97	42.33	-6.26	-0.01	-6.26	451.99
15	-6.44	19.10	-6.39	-0.05	-6.44	454.90

A = Est: free energy of binding (kcal/mol), B = Est. inhibition constant, Ki (mM), C = vdW + Hbond + desolv energy (kcal/mol), D = electrostatic energy (kcal/mol), E = total Intermolec. energy (kcal/mol), F = Interact. surface

Pharmacokinetic assessment

Various protocols have been employed over the years to predict pharmacokinetic parameters, including PKQuest [46, 47], PharmPK [48], and SwissADME [49, 50]. In this study, the pharmacokinetic properties of Dibenzo derivatives were evaluated using SwissADME software **(Table 5)**.

Table 5. Pharmacokinetic parameters involved in the chemical structure of dibenzo derivatives

Parameter	2	5	9	11	13	15
GI absorption	High	High	High	High	High	High
BBB permeant	No	Yes	Yes	Yes	Yes	Yes
P-GP substrate	No	Yes	Yes	Yes	No	No
CYP1A2 inhibitor	Yes	Yes	Yes	Yes	Yes	Yes
CYP2C19 inhibitor	Yes	No	No	No	Yes	Yes
CYP2C9 inhibitor	No	No	No	No	No	No
CYP2D6 inhibitor	No	No	No	No	No	No
CYP3A4 inhibitor	No	No	No	No	No	No

Pharmacokinetic evaluation

Various protocols have been used over the years to predict pharmacokinetic parameters, such as PKQuest, PharmPK, and SwissADME. In this study, we assessed the pharmacokinetic characteristics of Dibenzo derivatives using the SwissADME software **(Table 5)**. The analysis revealed differences in gastrointestinal absorption and metabolism, which may depend on the chemical structure of each Dibenzo derivative and its interaction with different cytochrome P450 systems.

Toxicity Evaluation

Some literature sources suggest that certain Dibenzo derivatives may exhibit toxicity in biological models. To assess this potential, the toxicity of Dibenzo derivatives (2, 5, 9, 11, 13, and 15) was evaluated using GUSAR

software. The results indicated that compound 5 required a higher dose to cause toxicity (LD50) through oral (2182 mg/kg) and intravenous (110.10 mg/kg) administration compared to other compounds. For example, compound 2 had an oral dose of 66.17 mg/kg and an intravenous dose of 1086 mg/kg, while compounds 9, 11, 13, and 15 exhibited varying levels of toxicity depending on the dose and route of administration. These findings suggest that toxicity is both dose- and route-dependent for these derivatives.

Conclusion

Theoretical assessments of dibenzo derivatives' interactions with the 4fdh protein suggest that derivatives 9, 11, and 15 may show a stronger affinity for the protein, which could enhance androgen receptor inhibition and potentially reduce prostate cancer levels. Additionally, compounds 2, 5, and 13 may act as 5α-reductase inhibitors, further contributing to prostate cancer inhibition.

Acknowledgments: None

Conflict of Interest: None

Financial Support: None

Ethics Statement: None

References

1. Pienta K, Gorin M, Rowe S, Carroll P, Pouliot F, Probst S. A phase 2/3 prospective multicenter study of the diagnostic accuracy of prostate-specific membrane antigen PET/CT with 18F-DCFPyL in prostate cancer patients (OSPREY). J Urol. 2021;206(1):52-61.
2. Lowrance W, Breau R, Chou R, Chapin B, Crispino T, Dreicer R, et al. Advanced prostate cancer: AUA/ASTRO/SUO guideline part I. J Urol. 2021;05(1):14-21.
3. Akhter S, Zain N, Shalauddin M, Singh V, Misnon I, Sharma R, et al. Tri-metallic Co-Ni-Cu based metal organic framework nanostructures for the detection of an anticancer drug nilutamide. Sens Act A Phys. 2021;325:112711.
4. Kim G, Song C, Yang Y, Lee N, Yoo H, Son S, et al. Chemical degradation of androgen receptor (AR) using bicalutamide analog– thalidomide PROTACs. Molecules. 2021;26(9):2525.
5. Leach D, Mohr A, Giotis E, Cil E, Isac A, Yates L, et al. The antiandrogen enzalutamide downregulates TMPRSS2 and reduces cellular entry of SARS-CoV-2 in human lung cells. Nat Comm. 2021;12(1):1-12.
6. Smith M, Saad F, Chowdhury S, Oudard S, Hadaschik B, Graff J, et al. Apalutamide and overall survival in prostate cancer. Eur Urol. 2021;79(1):150-8.
7. Goodman P, Tangen C, Darke A, Lucia M, Ford L, Minasian L, et al. Long-term effects of finasteride on prostate cancer mortality. New Eng J Med. 2019;380(4):393-4.
8. Hou Z, Huang S, Li Z. Androgens in prostate cancer: A tale that never ends. Cancer Lett. 2021;516:1-12.
9. Delaere K, Thillo E. Flutamide monotherapy as primary treatment in advanced prostatic cancer. Sem Oncol. 1991;18 (suppl 1):13-8.
10. Gomez J, Dupont A, Cusan L, Tremblay M, Tremblay M, Labrie F. Simultaneous liver and lung toxicity related to the nonsteroidal antiandrogen nilutamide (Anandron): a case report. Am J Med. 1992;92(5):563-6.
11. Boelsterli U, Ho H, Zhou S, Yeow K. Bioactivation and hepatotoxicity of nitroaromatic drugs. Curr Drug Metab. 2006;7(7):715-27.
12. Silva M, Souza J. Vulnerability of patients with prostatic hyperplasia treated with dutasteride and finasteride. Rev Bioética. 2021;29:394-400.
13. Eldhose B, Pandrala M, Xavier C, Mohamed A, Srivastava S, Sunkara A, et al. New selective inhibitors of erg positive prostate cancer: ERGi-USU-6 salt derivatives. Med Chem Lett. 2021;12(11):1703-9.
14. Xiang Q, Zhang Y, Li J, Xue X, Wang C, Song M, et al. Y08060: a selective BET inhibitor for treatment of prostate cancer. Med Chem Lett. 2018;9(3):262-7.
15. Ferroni C, Pepe A, Kim Y, Lee S, Guerrini A, Parenti M, et al. 1, 4- Substituted triazoles as nonsteroidal anti-androgens for prostate cancer treatment. Med Chem Lett. 2017;60(7):3082-93.

16. Baiz D, Pinder T, Hassan S, Karpova Y, Salsbury F, Welker M, et al. Synthesis and characterization of a novel prostate cancer-targeted phosphatidylinositol-3-kinase inhibitor prodrug. J Med Chem. 2012;55(18):8038-46.
17. Alagbala A, McRiner A, Borstnik K, Labonte T, Chang W, D'Angelo J, et al. Biological mechanisms of action of novel C-10 non-acetal trioxane dimers in prostate cancer cell lines. J Med Chem. 2006;49(26):7836-42.
18. Endo S, Oguri H, Segawa J, Kawai M, Hu D, Xia S, et al. Development of novel AKR1C3 inhibitors as new potential treatment for castration-resistant prostate cancer. J Med Chem. 2020;63(18):10396-411.
19. Adsule S, Barve V, Chen D, Ahmed F, Dou Q, Padhye S, et al. Novel Schiff base copper complexes of quinoline-2 carboxaldehyde as proteasome inhibitors in human prostate cancer cells. J Med Chem. 2006;49(24):7242-6.
20. Siddique H, Mishra S, Karnes R, Saleem M. Lupeol, a Novel Androgen Receptor Inhibitor: Implications in Prostate Cancer TherapyLupeol, a Novel Androgen Receptor Inhibitor. Clin Cancer Res. 2011;17(16):5379-91.
21. Ohtsu H, Xiao Z, Ishida J, Nagai M, Wang H, Itokawa H, et al. Antitumor agents. 217. Curcumin analogues as novel androgen receptor antagonists with potential as anti-prostate cancer agents. J Med Chem. 2002;45(23):5037-42.
22. Zhang Z, Connolly P, Lim H, Pande V, Meerpoel L, Teleha C, et al. Discovery of JNJ-63576253: a clinical stage androgen receptor antagonist for F877L mutant and wild-type castration-resistant prostate cancer (mCRPC). J Med Chem. 2021;64(2):909-24.
23. Stanisławska I, Granica S, Kiss A. Comparison of anti-proliferative effects of urolithins, ellagitannin gut metabolites, and non-steriodal antiandrogens on androgen-dependant prostate cancer cell line LNCaP. Planta Med. 2014;80(16):LP46.
24. Melkonyan F, Gevorgyan V. Catalytic Transformations via C-H Activation. Thieme. 2015;XV:5-69.
25. Yamada Y, Tanaka H, Kubo S, Sato S. Unveiling bonding states and roles of edges in nitrogen-doped graphene nanoribbon by X-ray photoelectron spectroscopy. Carbon. 2021;185:342-67.
26. Kargi F. Biological oxidation of thianthrene, thioxanthene and dibenzothiophene by the thermophilic organism Sulfolobus acidocaldarius. Biotechnol Lett. 1987;9(7):478-82.
27. Turner L. Interaction of Carmustine Tautomers with Adenine-DFT Study. Earth J Chem Sci. 2021;5(1):63-76.
28. Higgins S, Morris D, Muir K, Ryder K. The chiral oxime of 13 H- dibenzo (a, i) fluoren-13-one. Can J Chem. 2004;82(11):1625-8.
29. Aranda E, Kinne M, Kluge M, Ullrich R, Hofrichter M. Conversion of dibenzothiophene by the mushrooms Agrocybe aegerita and Coprinellus radians and their extracellular peroxygenases. Appl Microbiol Biotechnol. 2009;82(6):1057-66.
30. Jonas U, Hammer E, Schauer F, Bollag J. Transformation of 2- hydroxydibenzofuran by laccases of the white rot fungi Trametes versicolor and Pycnoporus cinnabarinus and characterization of oligomerization products. Biodegradation. 1997;8(5):321-7.
31. Khoshtariy T, Kakhabrishvili M, Kurkovskaya L, Suvorov N. Indolobenzofurans. 1. Synthesis of isomeric indolobenzo [b] furans. Chem Heter Comp. 1984;20(10):1123-7.
32. PatentScope (WIPO) SID 388542872. Available from: https://pubchem.ncbi.nlm.nih.gov/substance/388542872
33. PatentScope (WIPO) SID 388418871. Available from: https://pubchem.ncbi.nlm.nih.gov/substance/388418871
34. National Library of Medicine, PubChem. Available from: https://pubchem.ncbi.nlm.nih.gov/#query=dibenzo%5Ba%2Cc%5Dcycloheptene-5-carbonitrile
35. Vondráček J, Švihálková-Šindlerová L, Pěnčíková K, Krčmář P, Andrysík Z, Chramostová K, et al. 7H-Dibenzo [c, g] carbazole and 5, 9-dimethyldibenzo [c, g] carbazole exert multiple toxic events contributing to tumor promotion in rat liver epithelial 'stem-like' cells. Mutat Res/Fund Mol Mech Mutagen. 2006;596(1-2):43-56.
36. Moriconi E, Taranko L. Ozonolysis of polycyclic aromatics. XI. 1a 3- Methylcholanthrene2. J Org Chem. 1963;28(10):2526-9.

37. Sorrentino J, Orsi D, Altman R. Acid-Catalyzed Hydrothiolation of gem-Difluorostyrenes to Access α, α-Difluoroalkylthioethers. J Org Chem. 2021;86(3):2297-311.
38. Mihai D, Nitulescu G, Smith J, Hirsch A, Stecoza C. Dengue virus replication inhibition by dibenzothiepin derivatives. Med Chem Res. 2019;28(3):320-8.
39. Li J, Yu N, Guo H, Shi Y, Chen X, Wu J, et al. Combining virtual screening and in vitro evaluation for the discovery of potential CYP11B2 inhibitors. Future Med Chem. 2022;14(17):1239-50.
40. Prabhakar M, Mohanty A, Meena S. In silico screening of effective inhibitor of 5α-reductase type 1 for androgenic alopecia treatment. Nat Prod Res. 2021:1-6.
41. Figueroa L, Rosas M, Montserrat M, Díaz F, López M, Alvarez M, et al. Synthesis and theoretical interaction of 3-(2-oxabicyclo [7.4. 0] trideca-1 (13), 9, 11-trien-7-yn-12-yloxy)-steroid Deriva-tive with 17β-hydroxysteroid Dehydrogenase Enzyme Surface. Biointerface Res Appl Chem. 2023;13(3):266.
42. Lauro F, Marcela R, Maria L, Magdalena A, Virginia M, Francisco D, et al. Evaluation of biological activity of a diazocine derivative against heart failure using an ischemia-reperfusion injury model. Drug Res. 2021;72(07):404-11.
43. Gorla U, Rao K, Kulandaivelu U, Alavala R, Panda S. Lead finding from selected flavonoids with antiviral (SARS-CoV-2) potentials against COVID-19: an in-silico evaluation. Comb Chem High Thr Scr. 2021;24(6):879-90.
44. Sadashiva M, NanjundaSwamy S, Li F, Manu K, Sengottuvelan M, Prasanna D, et al. Anti-cancer activity of novel dibenzo [b, f] azepine tethered isoxazoline derivatives. BMC Chem Biol. 2012;12(1):1-11.
45. Desbois N, Pertuit D, Moretto J, Cachia C, Chauffert B, Bouyer F. cis- Dichloroplatinum (II) complexes tethered to dibenzo [c, h][1, 6] naphthyridin-6-ones: Synthesis and cytotoxicity in human cancer cell lines in vitro. Eur J Med Chem. 2013;69:719-27.
46. Lian J, Gao Y, Tang J, Chen X, Liu Y, Wu D, et al. Response of prostate cancer to addition of dutasteride after progression on abiraterone. Asian J Androl. 2021;23(2):222.
47. Levitt D. PKQuest: a general physiologically based pharmacokinetic model. Introduction and application to propranolol. BMC Clin Pharmacol. 2012;2(1):1-21.
48. Bourne D. Using the Internet as a pharmacokinetic resource. Clin Pharmacokinet. 1997;33(3):153-60.
49. Sicak Y. Design and antiproliferative and antioxidant activities of furan-based thiosemicarbazides and 1, 2, 4-triazoles: their structure-activity relationship and SwissADME predictions. Med Chem Res. 2021;30(8):1557-68.
50. Poland A, Glover E. Studies on the mechanism of toxicity of the chlorinated dibenzo-p-dioxins. Environ Health Perspect. 1973;5:245-51.